Chemical Engineering Journal 500 (2024) 157418

Contents lists available at ScienceDirect

Chemical Engineering Journal

journal homepage: www.elsevier.com/locate/cej

Strong self-healing close-loop recyclable vitrimers via complementary dynamic covalent/non-covalent bonding

Cheng Wang [a], Siqi Huo [b,d,*], Guofeng Ye [a], Qi Zhang [a], Cheng-Fei Cao [b], Mark Lynch [b,c], Hao Wang [b,d], Pingan Song [b,c,*], Zhitian Liu [a,*]

[a] Hubei Engineering Technology Research Center of Optoelectronic and New Energy Materials, School of Materials Science & Engineering, Wuhan Institute of Technology, Wuhan 430205, PR China
[b] Centre for Future Materials, University of Southern Queensland, Springfield 4300, Australia
[c] School of Agriculture and Environmental Science, University of Southern Queensland, Springfield 4300, Australia
[d] School of Engineering, University of Southern Queensland, Springfield 4300, Australia

ARTICLE INFO

Keywords:
Vitrimer
Room-temperature self-healing
Closed-loop recycling
Mechanical robustness
Fire retardancy

ABSTRACT

Epoxy vitrimers represent a new class of high-performance sustainable resins because of their desired mechanical and thermally malleable properties. Unfortunately, existing epoxy vitrimers cannot self-heal at room temperature (R.T.) due to the trade-off between mechanical robustness, recyclability, and the 'frozen' state of vitrimer networks at R.T. Herein, a high-performance hyperbranched epoxy vitrimer (DCNC/50PEDA) *via* curing bis(2,3-epoxypropyl) cyclohex-4-ene-1,2-dicarboxylate (DCNC) with 50 wt% of a phosphorus/silicon-containing polyethyleneimine (PEDA) at R.T., and the key to this design lies in rationally integrating complementary dynamic non-covalent hydrogen-bonding and π-π stacking and covalent β-hydroxy ester bonds into the high-mobility branched units of the DCNC/50PEDA network. This design endows the vitrimer with a room-temperature self-healing efficiency up to 96.0%, high mechanical strength reaching 36.0 MPa, and desired closed-loop recyclability. Moreover, its strong adhesion to a variety of substrates and exceptional fire retardancy, e.g., a limiting oxygen index of 39.0% and a desired UL-94 V-0 rating, make it an outstanding fire-retardant coating for flammable substrates, such as wood. Such a performance portfolio enables DCNC/50PEDA to outperform existing self-healing polymer and vitrimers counterparts. This work establishes a promising complementary dynamic design protocol for creating self-healing, strong, recyclable, and fire-safe polymers by integrating dynamic non-covalent interactions and covalent bonds, which hold great real-world applications in industries, such as bulk materials, coatings, and adhesives.

1. Introduction

Synthetic polymers are widely used in society but increasingly a range of serious environmental issues are observed, particularly plastic pollution, which is due to inability of these materials to break down in natural environments [1]. Vitrimers, as a new class of polymeric materials, have recently emerged and present innovative opportunities to address the waste plastic issue [2,3]. Because of the presence of dynamic covalent networks, vitrimers combine the dual advantages of thermosets and thermoplastics [4,5], such as good mechanical properties, weldability, reprocessability, and recyclability [6,7]. Epoxy vitrimers show great promise due to ease of preparation, low cost, and great overall performance [8–10]. Thus, epoxy vitrimers have great potential to replace traditional epoxy thermosets in a range of applications, such as construction, aerospace, and electronic devices [7,11].

Unfortunately, most existing epoxy vitrimers have some shortcomings, particularly their healing performances. Typically, external stimuli, such as light, heat, and chemicals agents, are often required to induce exchange reactions between dynamic covalent bonds within their topological network to achieve remoldability and recyclability [12,13]. This means epoxy vitrimers are generally unable to heal without external stimuli [14]. Unlike epoxy vitrimers, the healing process of self-healing polymers mainly relies on their dynamic noncovalent bonds, and often involves chain diffusion, dynamic noncovalent bond

* Corresponding authors at: Centre for Future Materials, University of Southern Queensland, Springfield 4300, Australia (S. Huo).
E-mail addresses: sqhuo@hotmail.com, Siqi.Huo@unisq.edu.au (S. Huo), pingansong@gmail.com, pingan.song@usq.edu.au (P. Song), able.ztliu@wit.edu.cn (Z. Liu).

https://doi.org/10.1016/j.cej.2024.157418
Received 16 July 2024; Received in revised form 22 October 2024; Accepted 3 November 2024
Available online 4 November 2024

reassociation, and chain entanglement [6,15–17]. Because such healing processes require high molecular or chain mobility, to date room-temperature self-healing has only been reported in soft polymers, such as elastomers and hydrogels with glass transition temperatures (T_gs) lower than room temperature.

As typical glassy polymers, epoxy vitrimers normally have T_g values much higher than room temperature (R.T., ~25 °C) [18–20], making self-healing impossible at R.T. due to the trade-off between self-healing and mechanical properties (stiff epoxy chains) [15,21,22]. The high mechanical strength and modulus of epoxy vitrimers primarily originates from its strong internal interaction forces and high cross-linking density. The highly cross-linked networks in epoxy vitrimers significantly restrict the movement and conformational transitions of the chain segments, leading to an inability to self-heal at R.T. Therefore, it is challenging to develop advanced epoxy vitrimers that combine room-temperature self-healing, recyclability, and high mechanical strength.

Apart from high mechanical strength and self-healing capabilities, it is equally important to impart good flame retardance to epoxy vitrimers

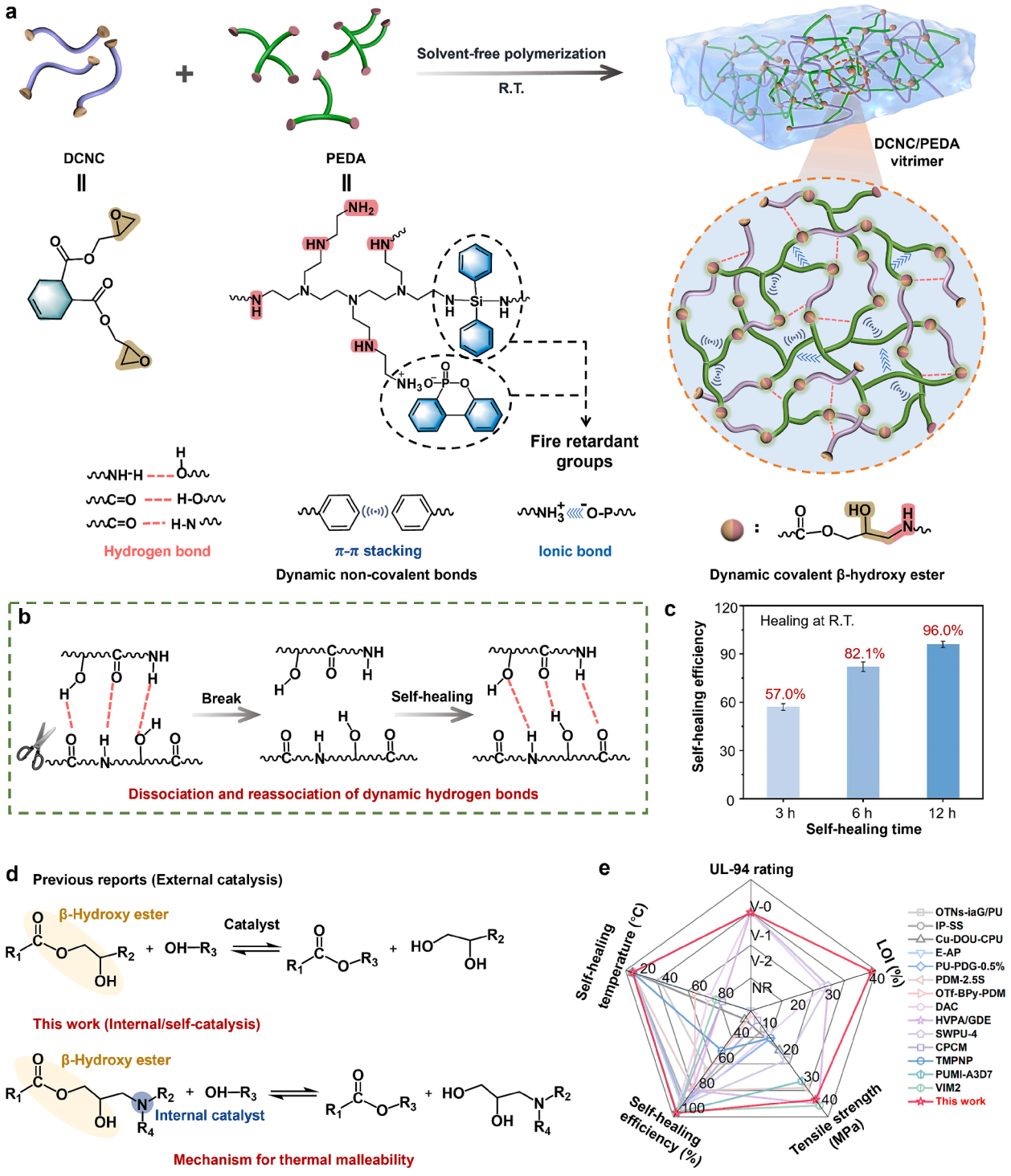

Fig. 1. Rational design and synthesis of DCNC/PEDA vitrimer. (a) Schematic illustration for the synthesis of DCNC/PEDA vitrimer. (b) the self-healing mechanism and (c) self-healing efficiency as a function of healing time for DCNC/50PEDA vitrimer. (d) the molecular mechanism of thermal malleability. and (e) the comparison of self-healing, mechanical, and fire-retardant properties of the DCNC/50PEDA vitrimer compared to other self-healing polymers and vitrimers.

to ensure their versatility in real-world applications [23,24]. Previous work has shown that the use of phosphorus (P)-containing hardeners can also impart intrinsic fire retardancy to EP [25–27]. The introduction of additional fire-retardant elements, such as silicon (Si), boron (B), and nitrogen (N), as P-based curing/co-curing agents can further boost the fire retardance by way of synergistic effects [28,29]. Therefore, the design of multiple element-containing fire-retardant hardeners is a promising strategy for creating high-strength room-temperature self-healing epoxy vitrimers.

Herein, we report a high-performance hyperbranched epoxy vitrimer (DCNC/50PEDA) by a complementary dynamic design strategy, and the key to this design lies in the integration of complementary dynamic non-covalent hydrogen bonding/π-π stacking with covalent β-hydroxy ester bonds into the branched units of the vitrimer network. With this rational design, as-prepared vitrimer exhibits an ability to self-heal at R.T., robust mechanical properties, closed-loop recyclability, and intrinsic fire retardancy. The DCNC/50PEDA vitrimer exhibits a room-temperature self-healing efficiency as high as 96.0%. This is because upon damage, the hyperbranched chains can easily diffuse to the interface at R.T., leading to the reformation of hydrogen-bonding/π-π stacking interactions to ultimately achieve chain entanglement and self-repair. The vitrimer displays a high tensile strength and outstanding fire retardancy, with strong adhesion to various substrates. Thus, it can serve as an effective fire-retardant coating for flammable substrates, such as timber. This performance portfolio makes it superior to previous room-temperature self-healing polymers. The resultant epoxy vitrimers hold great potential for practical applications in various industries, such as construction, coatings, and adhesives.

2. Experimental section

This is provided in the Supporting Information.

3. Results and discussion

3.1. Preparation and characterization

The preparation of the DCNC/50PEDA vitrimer is achieved by a solvent-free polymerization between epoxy monomer (DCNC, addition: 50 wt%) and a P/Si-containing polyethyleneimine-based curing agent (PEDA, addition: 50 wt%) at R.T. (see Fig. 1a and Fig. S1 and Table S1). The PEDA was synthesized from dibenzo[c,e][1,2]oxaphosphinic acid (DOPA), polyethylenimine (PEI), and dichlorodiphenylsilane. Its chemical structure was confirmed by ^{1}H and ^{31}P nuclear magnetic resonance (NMR), gel permeation chromatography (GPC) and Fourier transform infrared (FTIR) spectroscopy (see Fig. S2). Because of abundant dynamic hydrogen bonding and π-π stacking within its high-mobility branched units, the as-synthesized DCNC/50PEDA features an extraordinary room-temperature self-healing ability (see Fig. 1b). Based on the change in tensile strength, the DCNC/50PEDA vitrimer shows a self-healing efficiency up to 96.0% at R.T. over 12 h (see Fig. 1c). Moreover, DCNC/50PEDA is also physically/chemically a closed-loop recyclable due to its secondary and tertiary amine groups that serve as internal catalysts to facilitate the transesterification of β-hydroxy esters, which ultimately results in topological rearrangement (see Fig. 1d). In brief, the as-designed DCNC/50PEDA vitrimer exhibits a high room-temperature self-healing efficiency and closed-loop recyclability.

We examined the comprehensive physical performances of the as-prepared DCNC/50PEDA vitrimer. It shows a gel fraction as high as 93.7% by equilibrium swelling testing (see Table S2). DCNC/50PEDA presents a glass transition temperature (T_g) of 52.1 °C, which is higher than 46.4 °C of the PEI-cured DCNC (DCNC/50PEI), and it also exhibits a higher cross-linking density (see Fig. S3 and Table S1). This is mainly due to the presence of rigid P- and Si-containing groups, thus rendering DCNC/50PEDA to behave like a glassy polymer at room temperature. Meanwhile, the DCNC/50PEDA shows robust mechanical properties, with tensile strength and elongation at break reaching 36.0 MPa and 51.3%, respectively, which are higher than corresponding values of DCNC/50PEI (see Fig. S4). Such robust mechanical properties can be attributed to the presence of rigid groups and the formation of hydrogen and ionic bonds, and π-π stacking.

Additionally, the DCNC/50PEDA exhibits high transparency and good UV-shielding performance, which is advantageous for its practical applications. Its film (thickness: 500–600 μm) has high transparency at 800 nm, suggesting that the presence of phosphorus- and silicon-based groups does not affect the transparency of the vitrimer (see Fig. S5a-c) [25]. The film does show a lower transmittance, producing an ultraviolet protection factor (UPF) of 27.5 due to the presence of benzene-rich groups (see Fig. S5b and d). Along with a surface energy of 19.9 MJ/m^2 (see Table S2), the DCNC/50PEDA exhibits oil–water contact angles reaching 98.7° and 103.2°, respectively (see Fig. S6), which is indicative of its intrinsic hydrophobicity and oleophobicity. The DCNC/50PEDA gives an initial decomposition temperature ($T_{5\%}$, corresponding to 5 % weight loss) at 221 °C in N_2 condition, and 172 °C in air (see Table S3), indicative of its thermal stability. Because of the high charring ability of PEDA (see Fig. S7 and Table S3), the DCNC/50PEDA shows much higher char yield (*CY*) values than DCNC/50PEI (see Fig. S8). Specifically, the *CY* values of DCNC/50PEDA increase from 0.6 % and 0.1 % of DCNC/50PEI to 13.7% (in N_2) and 7.9% (in air) or by about 22– and 78-fold. Because of the presence of P- and Si-containing groups, the DCNC/50PEDA shows a high LOI value of 39.0% and desired UL-94 V-0 rating, (see Fig. S9), suggesting exceptional intrinsic fire retardance. The comprehensive performances of DCNC/50PEDA vitrimer were compared to previously reported self-healing polymers and vitrimers. As shown in Fig. 1e and Table S4 [30–43], besides excellent fire retardancy, as-prepared DCNC/50PEDA vitrimer shows an unprecedented performance spectrum, including a room-temperature self-healing efficiency of 96.0%, and a tensile strength of 36.0 MPa, surpassing its counterparts.

3.2. Self-healing performances

In real-world applications, materials are often susceptible to different types of damage, such as cuts, punctures, and scratches [44]. Hence, we examine the room-temperature self-healing performances of DCNC/50PEDA due to different damage (see Fig. 2a-c). A clean blade was applied to cut a notch with a width of ~110 μm on the film surface, and the self-healing process at R.T. of DCNC/50PEDA was observed by optical microscopy. The notch width gradually reduced over time and decreased to ~20 μm after 6 h of healing, disappearing completely within 12 h (see Fig. 2a_1-a_3). In addition, the self-healing processes of DCNC/50PEDA were also assessed after being punctured and scratched by both a needle and abrasive paper. As presented in Fig. 2b_1-b_3 and c_1-c_3, both holes (width: ~10 μm) and scratches on the DCNC/50PEDA surface can fully heal after being left at R.T. for 12 h. These results clearly demonstrate an outstanding room-temperature self-healing capability of as-developed DCNC/50PEDA vitrimer without any external stimuli, which can significantly extend its lifespan in many harsh industrial settings.

To quantitatively evaluate the self-healing performance of DCNC/50PEDA vitrimer, tensile testing was conducted on the healed specimens. The self-healing efficiency is defined as the ratio of the tensile strength of the healed specimen to the original specimen [45]. Fig. 2d and e show the tensile stress–strain curves of the cut and punctured DCNC/50PEDA vitrimer before and after self-healing. Upon a cut damage, the tensile strength of DCNC/50PEDA reduces from 36.0 MPa to 11.2 MPa. Its tensile strength recovers to 20.5 and 29.5 MPa, respectively after self-healing at R.T. for 3 and 6 h, and reaches 34.6 MPa after 12 h, leading to a self-healing efficiency as high as 96.0% (see Fig. 2d and f). Likewise, the tensile strength of the punctured DCNC/50PEDA recovers from 16.5 to 34.8 MPa after 12 h of healing at 25 °C, giving rise to a high self-healing efficiency of 96.7% (see Fig. 2e and f). The results

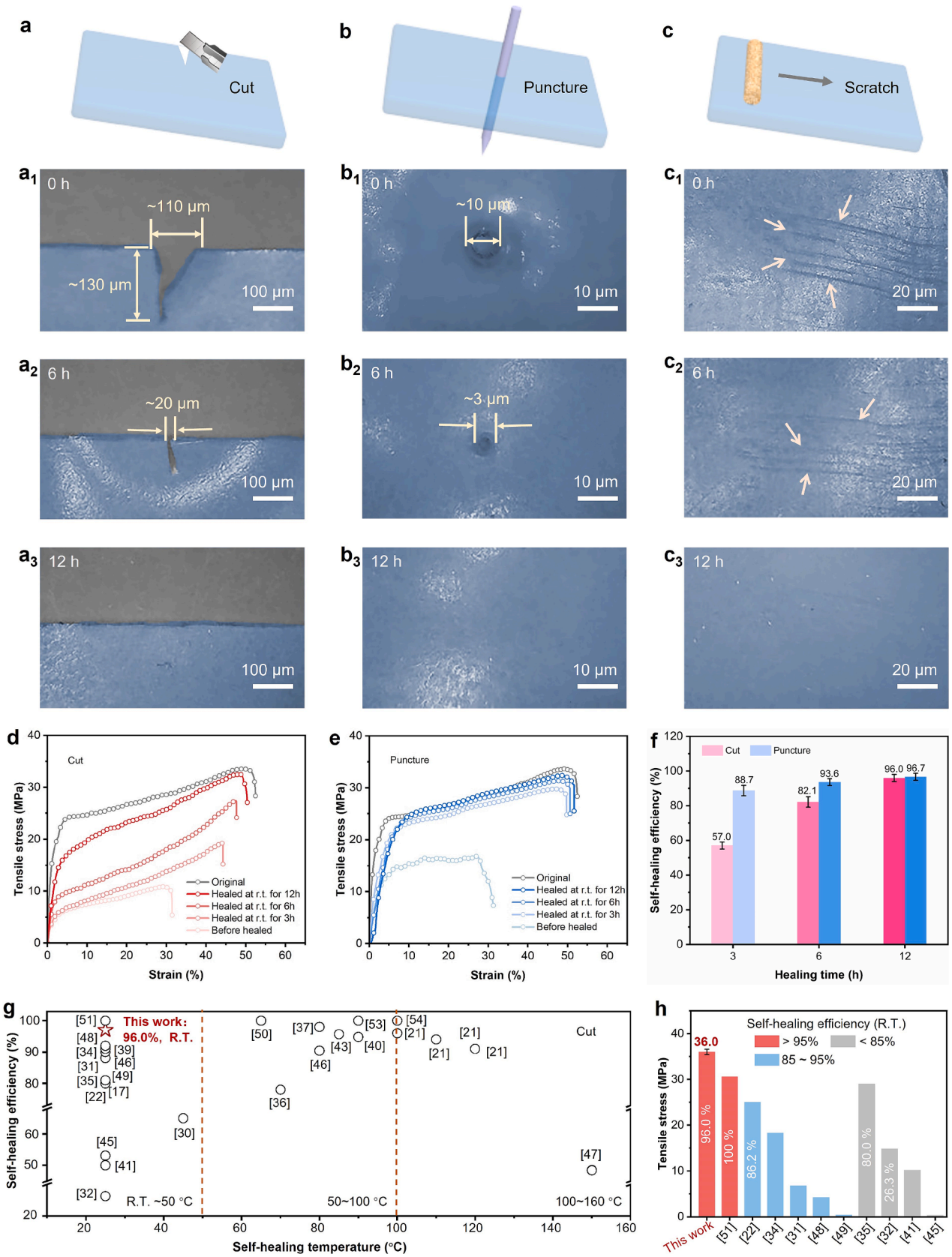

Fig. 2. Self-healing performances of DCNC/50PEDA vitrimer after different damage modes. Schematic illustration for (a) cut, (b) puncture, and (c) scratch damage. the self-healing process at R.T. after (a_1-a_3) cut, (b_1-b_3) puncture, and (c_1-c_3) scratch damage. the tensile stress–strain curves of (d) cut and e) punctured DCNC/50PEDA after healing for different time at R.T. (f) the self-healing efficiency after healing for different time at R.T. (g) the self-healing efficiency/temperature comparison between DCNC/50PEDA vitrimer and previous self-healing polymers. and (h) tensile strength and self-healing efficiency comparison of DCNC/50PEDA vitrimer and previously-reported room-temperature self-healing polymers.

strongly confirm the superior room-temperature self-healing property of DCNC/50PEDA. In addition, with increasing healing temperature, the self-healing efficiency of DCNC/50PEDA increases, and a shorter healing time is required (see Fig. S10). For instance, after being repaired for 3 h at 60 and 80 °C, the self-healing efficiency of the cut DCNC/50PEDA reaches 89.6 and 97.9%, respectively and that of the punctured material is up to 93.1 and 98.1%. The increased self-healing efficiency is attributed to the chain segment diffusion and dynamic exchange reactions

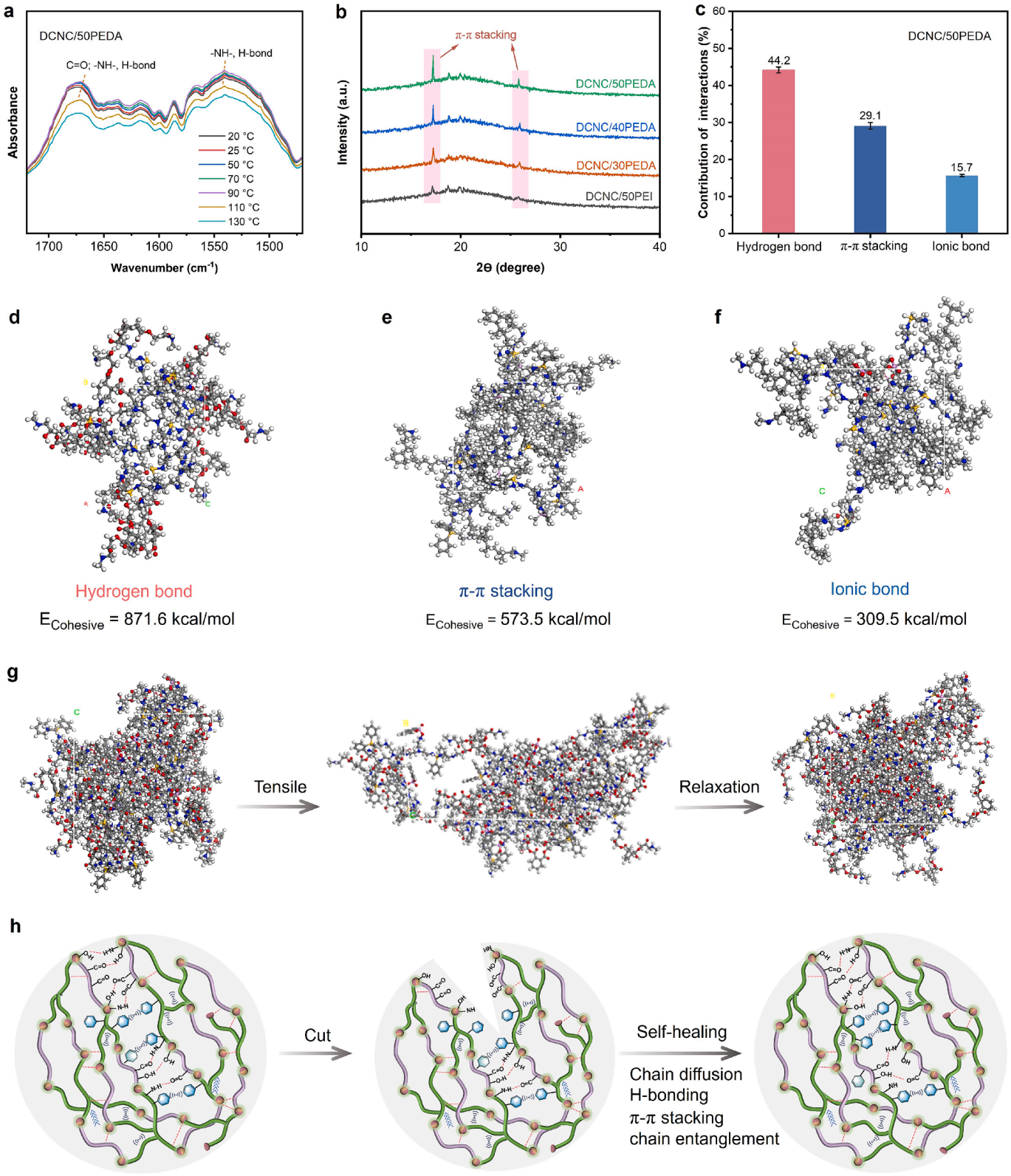

Fig. 3. The self-healing mechanism of DCNC/50PEDA vitrimer. (a) Temperature-dependent FTIR spectra from 20 to 130 °C. (b) XRD patterns of DCNC/50PEI and DCNC/PEDA samples at 25 °C. (c) the contribution of interactions, the construction model for calculating the cohesive energy of (d) hydrogen bond, (e) π-π stacking, and (f) ionic bond. (g) the tensile and relaxation process. and (h) schematic illustration of the self-healing mechanism.

within the cross-linking network which are faster at elevated temperatures [42].

Compared with previous self-healing polymers [17,21,22,30–32,34–43,45–53], the DCNC/50PEDA vitrimer exhibits superior self-healing properties in terms of self-healing temperature and efficiency (see Fig. 2g and Table S4). As-fabricated DCNC/50PEDA shows higher self-healing efficiency (96.0%) and tensile strength (36.0 MPa) than previous room-temperature self-healing polymers (see Fig. 2h and Table S4). In brief, our DCNC/50PEDA vitrimer realizes the unique combination of high mechanical strength, low healing temperature and high healing efficiency as well as exceptional fire retardance.

3.3. Self-healing mechanism

3.3.1. Experimental validation

Generally, self-healing materials primarily rely on chain segment movement, diffusion, rearrangement, and entanglement on their cross-section to achieve self-healing [19,44]. Since the DCNC/50PEDA is a glassy polymer, its chain mobility and diffusion characteristics are severely limited at R.T. Theoretically, it is unlikely to achieve self-healing at R.T. but as-prepared DCNC/50PEDA can almost fully self-repair in 12 h at R.T. For this reason, it is essential to elucidate its self-healing mechanism.

The room-temperature self-healing performance of the DCNC/50PEDA is related to its non-covalent interactions between chain segments within its cross-linking network. The FTIR spectrum reveals the existence of abundant hydrogen bonds (H-bonds) formed between –NH-, –OH, and C=O groups in the cross-linking network of the DCNC/50PEDA (see Fig. S11). In the temperature-dependent FTIR spectra, there are two broad peaks at 1675 and 1544 cm^{-1} belonging to C=O and –NH- groups, respectively, which are involved in the H-bonding [54] (see Fig. 3a). When the temperature increases from 25 to 90 °C, these two peaks gradually redshift to 1670 and 1540 cm^{-1}, which shows the enhanced H-bonding interactions. However, these two peaks begin to blueshift to 1673 and 1542 cm^{-1} with a further increase in temperature, which is indicative of the gradual dissociation of H-bonds [34]. This is because with increasing temperature, the movement of chain segments are activated, which gives rise to the formation of more H-bonds. However, at higher temperatures chain segments move too fast, which leads to dissociation of H-bonds. The X-ray diffraction (XRD) patterns (see Fig. 3b) show two diffraction peaks centered at 17.2 and 25.2°, indicating the formation of π-π stacking arising from cyclohexene and benzene groups within the cross-linking networks of both DCNC/50PEDA and DCNC/50PEI [55]. Compared with DCNC/50PEI, the DCNC/PEDA samples exhibit stronger π-π stacking due to the introduction of benzene ring from PEDA, and the π-π stacking of DCNC/PEDA is gradually enhanced with the increase of PEDA content. In addition, Compared to DCNC/50PEI, the DCNC/50PEDA shows a characteristic peak of NH_3^+ group at 1530 cm^{-1} in its IR spectrum (see Fig. S12), indicating the presence of ionic bonds in the network [56]. In summary, both the H-bonding and π-π stacking interactions in the cross-linked network are responsible for the excellent room-temperature self-healing property of the DCNC/50PEDA.

To further understand the healing mechanism of the DCNC/50PEDA, its dynamic response was also investigated by dynamic mechanical analysis (DMA), where the stress relaxation and storage curves (see Fig. S13) are obtained based on tensile and single cantilever modes, respectively. The relaxation time (τ), defined as the time for the normalized stress to drop to 1/e, of the vitrimer is a specific parameter to characterize the rate of bond-exchange reactions within the network [57]. Like the DCNC/50PEI, the τ value of the DCNC/50PEDA decreases with increasing temperatures, eventually reduces to 10.6 min at 120 °C, indicating fast stress relaxation even without using an external catalyst (see Fig. S13a and b). Notably, the τ value of the DCNC/50PEDA is much lower than that of DCNC/50PEI, probably because of the abundant H-bonds and π-π stacking which can facilitate the movement of chain segments, and thus accelerate the bond-exchange reactions. Additionally, the linear correlation between ln(τ) with 1000/T reveals the Arrhenius flow characteristics of the DCNC/50PEDA network (see Fig. S13c) [58]. Based on Equation (4) in the Supporting Information, the activation energy of the ester exchange reaction within the DCNC/50PEDA is calculated to be 106 kJ/mol, consistent with the reported 69–150 kJ/mol by others [5], which further confirms that the DCNC/50PEDA is a vitrimer. To further explore its vitrimer characteristics further, it was soaked in *N*-Methyl-2-pyrrolidone (NMP) and NMP/ethylene glycol (EG) with a volume ratio of 4:1, at 120 °C for 6 h (see Fig. S14). After 6 h, the DCNC/50PEDA specimen was only partially dissolved in NMP, but completely dissolved in NMP/EG. This result demonstrates that the as-prepared DCNC/50PEDA is a transesterification vitrimer, since EG molecules accelerate its decomposition.

According to Fig. S13c and d and Equation (5) and (6) in the Supporting Information, the DCNC/50PEDA shows a topology freezing transition temperature (T_v) of 41 °C, which means that its transesterification reactions are largely frozen at R.T. This further manifest in its room-temperature self-healing ability which is mainly attributed to the dynamic H-bonds and π-π stacking within its network. In addition, at R.T., the DCNC/50PEDA exhibits a τ of e^{12} s (see Fig. S13c), which is much lower than e^{23} s of the DCNC/50PEI. According to previous work [59], the branched chain segments of a hyperbranched polymer are highly migratory. Presumably, the branched chains of the DCNC/50PEDA easily diffuse across the damaged interface after damage, which then entangle with other chain segments to reconstruct the noncovalent network driven by dynamic H-bonds and π-π stacking, thus leading to self-healing at room temperature.

3.3.2. Molecular dynamics simulation

Molecular dynamics (MD) simulations have been widely utilized to investigate the self-healing behaviors of polymers. The cohesive energy and contribution of H-bonding, π-π stacking and ionic bonds within the DCNC/50PEDA network were calculated by removing irrelevant groups in the simulated system (see corresponding models in Fig. S15 and S16). All-atom MD simulations reveal that the cohesive energy of H-bonding, π-π stacking and ionic bonds are 871.6, 573.5 and 309.5 kcal/mol, respectively (see Fig. 3d and f). Based on the total cohesive energy of the DCNC/50PEDA (1974.4 kcal/mol), the contributions of H-bonding, π-π stacking, and ionic bonds were calculated to be 44.2%, 29.1%, and 15.7%, respectively, indicating that H-bonding within the DCNC/50PEDA network plays a dominant role, followed by π-π stacking (see Fig. 3c). This further proves that both H-bonding and π-π stacking are mainly responsible for the room-temperature self-healing ability of as-developed DCNC/50PEDA.

A stress–strain model was used to analyze the motion trajectories of the DCNC/50PEDA chains to show the chain movement, with the representative trajectories in Fig. 3g and the integrated trajectories in Fig. S17. Upon stretching by external forces, the chain segments in the DCNC/50PEDA gradually cohere, and finally return to the equilibrium state. The number of H-bonds gradually increases instead of reducing when the chains are stretched under external forces. This is probably because the chains of the DCNC/50PEDA are in a frozen state at R.T., and the external forces promote chain segment motion, leading to the formation of more H-bonds. During the relaxation process, the number of H-bonds gradually reduces, and eventually becomes equivalent to the original state. This further confirms that dynamic H-bonding plays a critical role in the room-temperature self-healing of DCNC/50PEDA. Driven by abundant H-bonding and π-π stacking interactions, the branched units or chain segments within the DCNC/50PEDA network can diffuse across the interface and become entangled with each other, thereby achieving self-healing in response to damage (see Fig. 3h).

3.4. DCNC/50PEDA as high-performance adhesive/coating

In addition, we also evaluated the chemical resistance, adhesion

properties, and physical/chemical recyclability of as-prepared DCNC/50PEDA vitrimer as adhesive/coating to demonstrate its practical applications in industry settings. As a coating/adhesive, polymeric materials are expected to show excellent chemical resistance, but most vitrimers cannot meet this requirement because of their dynamic cross-linked networks. As-prepared DCNC/50PEDA exhibits strong solvent resistance and chemical stability. No obvious change in its structure and solvent color are observed after DCNC/50PEDA is immersed in 1.0 mol/L NaOH solution, or 1.0 mol/L HCl solution for 168 h, which is indicative of its good acid and alkali tolerance (see Fig. S18 and S19). Moreover, its gel fraction is higher than 90%, and thus the swelling rate is lower than 10% after soaked in a range of different solvents for 168 h (see Table S5). This demonstrates its excellent chemical stability and acid/alkali resistance, which is superior to many previously-reported transesterification vitrimers [58,60,61].

We also examined the adhesive performances of DCNC/50PEDA on different substrates, including wood, ceramic, copper, steel, glass, thermoplastic polyurethane (TPU), and polytetrafluoroethylene (PTFE). Wood bonded with only 0.1 g of DCNC/50PEDA adhesive can lift an item weighting 10 kg, which is indicative of excellent peel resistance, as shown in Fig. 4a. The DCNC/50PEDA presents high shear strength on different substrates (see Fig. 4b), with an order: wood (8.7 MPa) > ceramic (4.4 MPa) > copper (2.7 MPa) > steel (2.4 MPa) > glass (2.1 MPa) > TPU (1.1 MPa) > PTFE (0.1 MPa). These results show that the DCNC/50PEDA vitrimer can adhere to a variety of substrate materials, from metals and inorganic nonmetallic materials to organic polymers, due to its strong noncovalent interactions. It is worth noting that the adhesion strength of DCNC/50PEDA on wood is higher than 8.7 MPa since it is at this point the wood breaks before failure of adhesion interfaces is observed (see Fig. S20). Compared to existing adhesives/coatings for wood (see Ref. S11-S19 in the Supporting Information), as-prepared DCNC/50PEDA shows higher adhesive strength, outperforming its counterparts (see Fig. 4c and Table S6). In addition, the adhesion strength of DCNC/50PEDA is only slightly reduced (retention rate: >91%) after undergoing different aging tests (e.g., heat, hydrothermal, HCl, NaOH, and UV-light) for 168 h (see Fig. S21). It still maintains strong adhesion to a variety of substrates, even after outdoor exposure for 720 h (see Fig. S21), strongly suggesting the durability of its adhesion properties.

To better understand the adhesion mechanism of the DCNC/50PEDA, density functional theory (DFT) was used to calculate the interaction energy between it and wood/TPU/steel (see Fig. S22 and S23). The interaction energy of DCNC/50PEDA with wood is up to –322.4 kcal/mol, significantly higher than that with TPU (−68.8 kcal/mol) and steel (−179.5 kcal/mol), further highlighting its stronger adhesion to wood. Thus, combined with molecular dynamics simulations, the effective adhesion of DCNC/50PEDA was attributed to three aspects. One is the cohesive energy, which mainly consists of intermolecular hydrogen bonding. The other is the interfacial energy, which mainly composed of interfacial hydrogen bonding and adsorption of metal atoms. And the last is that the hyperbranched structure of PEDA can effectively dissipate energy to resist internal crack extension under external force. This means that the ester, amine, and hydroxyl groups in the DCNC/50PEDA can form abundant H-bonding with wood, and TPU, while with metal substrates there is the possibility of forming coordination bonds. This results in high interaction energy and strong adhesion toward a range of substrates (see Fig. S24).

As-developed DCNC/50PEDA can be recycled and reused through simple physical means because of its autocatalytic transesterification reaction (see Fig. 4d and g). To assess its reusability, the damaged single-lap shear specimen is hot-pressed at different temperatures, and the lap shear strength of the DCNC/50PEDA to copper and steel after physical recycling is tested. The adhesion strength of the DCNC/50PEDA after being reconditioned at 100 °C for 30 min is as high as 2.6 MPa (to copper) and 2.3 MPa (to steel), respectively, which are very close to their original values (see Fig. 4e). Even if the hot-pressing temperature reduces to 60 °C, the shear strength of the DCNC/50PEDA on copper and steel can still reaches 2.0 and 1.9 MPa, respectively, indicating that its adhesion properties can be quickly restored in mild conditions. Moreover, the recovery rates of its adhesive strength to copper and steel can reach 96 and 94% after being recycled 5 times (see Fig. 4f). These results clearly demonstrate the closed-loop recyclability of DCNC/50PEDA.

DCNC/50PEDA can also be recycled by chemical methods. As shown in Fig. 4g, it can be completely decomposed into cyclohex-4-ene-1,2-dicarboxylic acid, and PEDA derivatives after being soaked in 1 mol/L NaOH aqueous solution at 80 °C for 6 h (see Fig. S25). Both products can be readily separated by treatment with 1 mol/L of HCl, and ethanol, with yields up to 96%. The chemical structures of cyclohex-4-ene-1,2-dicarboxylic acid and PEDA derivative were confirmed by ^{1}H NMR, ^{31}P NMR and FTIR (see Fig. 4h and 4i, Fig. S26 and S27). For PEDA derivatives, the signals at 6.9–7.9 ppm and 8.5 ppm are attributed to the protons of aromatic groups, and hydroxyl groups respectively (see Fig. S26). Only one peak is observed in the ^{31}P NMR of PEDA derivative, and its chemical shift (1.02 ppm) is close to the peak (0.85 ppm) in the ^{31}P NMR of PEDA (see Fig. 4i). For cyclohex-4-ene-1,2-dicarboxylic acid, the chemical shifts between 7.0–8.0 ppm in its ^{1}H NMR are attributed to the protons of –CH_2- and –CH=CH– groups (see Fig. 4h).

The peaks at 1450 and 1240 cm^{-1} in the FTIR spectrum of PEDA derivative are assigned to benzene ring and P=O bonds, and the absorption peaks located at 1730 and 1670 cm^{-1} are attributed to C=O and C=C groups in cyclohex-4-ene-1,2-dicarboxylic acid (see Fig. S27). These results suggest that the DCNC/50PEDA vitrimer can be chemically degraded into cyclohex-4-ene-1,2-dicarboxylic acid, and PEDA derivatives (see Fig. 4j). Moreover, both recycled products have high purity, and can also be reused to prepare the DCNC/50PEDA vitrimer by curing at 60 °C for 3 h. Notably, the adhesion strength of the recycled DCNC/50PEDA vitrimer to different substrates almost retains the original values, even after being chemically recycled 5 times, with the recovery rate of the adhesion strength of ≥99% (see Fig. 4k). Hence, as-developed DCNC/50PEDA features satisfactory chemical resistance, high adhesion strength, and desired closed-loop recyclability, and thus shows great potential as a high-strength recyclable adhesive.

3.5. DCNC/50PEDA as fire-retardant coating for wood

Wood is extensively used in construction due to its renewability, carbon neutrality, and high specific strength, but suffers from high flammability, and thus fire-retardant treatments are necessary in a range of applications. Since our DCNC/50PEDA features great fire retardancy and strong adhesion to wood, we have explored the potential of DCNC/50PEDA as a fire-retardant coating for wood. Although only a ~40 μm thick DCNC/50PEDA coating was applied onto the wood surface as determined by scanning electron microscopy (SEM) (see Fig. 5a), the treated wood achieves satisfactory fire retardance. Specifically, the uncoated wood shows a low LOI of 20.0%, and completely burns out 60 s after the first ignition (see Fig. 5b) during UL-94 testing, indicating its high flammability. In comparison, the coated wood acquires a high LOI value of 30.0%, and moreover, it can immediately self-extinguish after the removal of the ignition source, leading to a desired UL-94 V-0 rating during vertical burning testing, strongly indicative of its improved fire retardancy (see Fig. 5c and d). Additionally, the coated wood shows much lower heat release rates than untreated wood and wood coated with DCNC/50PEI (see Fig. S28a and b and Table S8).

The DCNC/50PEDA-treated wood shows durable flame retardancy as evidenced by the unchanged LOI value and UL-94 rating after exposure to different aging conditions, such as heat, HCl, NaOH, and UV-light, for 168 h (see Fig. 5e). Also, the wood treated with reproduced DCNC/50PEDA after 5 cycles of chemical recycling still maintains the same fire-retardant properties (see Fig. 5f). The DCNC/50PEDA coating features noticeable advantages over previously reported fire-retardant coatings for wood (Supplementary Ref. 20-30), in terms of achieving a high LOI value of 30% and a UL-94 V-0 classification at an ultra-thin thickness of

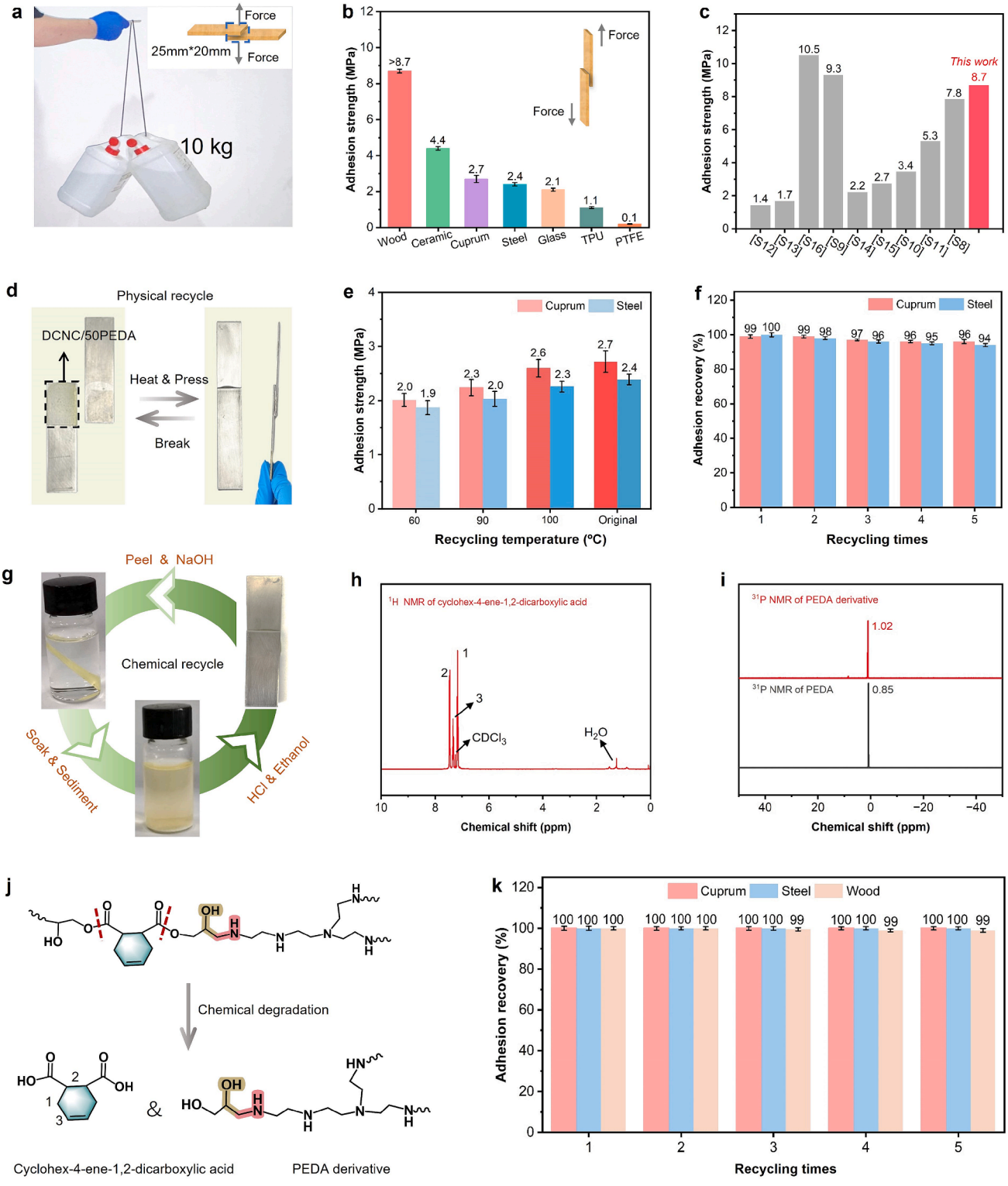

Fig. 4. The performances of DCNC/50PEDA adhesive/coating. (a) Schematic illustration of the fabrication of lap shear specimen using DCNC/50PEDA as adhesive. (b) adhesion strength on different substrates. (c) adhesion strength comparison between DCNC/50PEDA and previous adhesives towards wood. (d) schematic of physical recycling process (by hot-pressing). (e) adhesion strength (towards steel and cuprum) of reused DCNC/50PEDA achieved by hot-pressing for 30 min at different temperatures. (f) recovery percentage (in terms of adhesive strength) of DCNC/50PEDA after different physical recycling times (recycling method: hot-pressing at 60 °C for 2 h). (g) schematic of chemical recycling process. (h) ^{1}H NMR of cyclohex-4-ene-1,2-dicarboxylic acid and (i) ^{31}P NMR of PEDA derivative. (j) chemical degradation products of DCNC/50PEDA vitrimer, and (k) recovery percentage (in terms of adhesive strength) of DCNC/50PEDA on different substrates after different chemical recycling cycles.

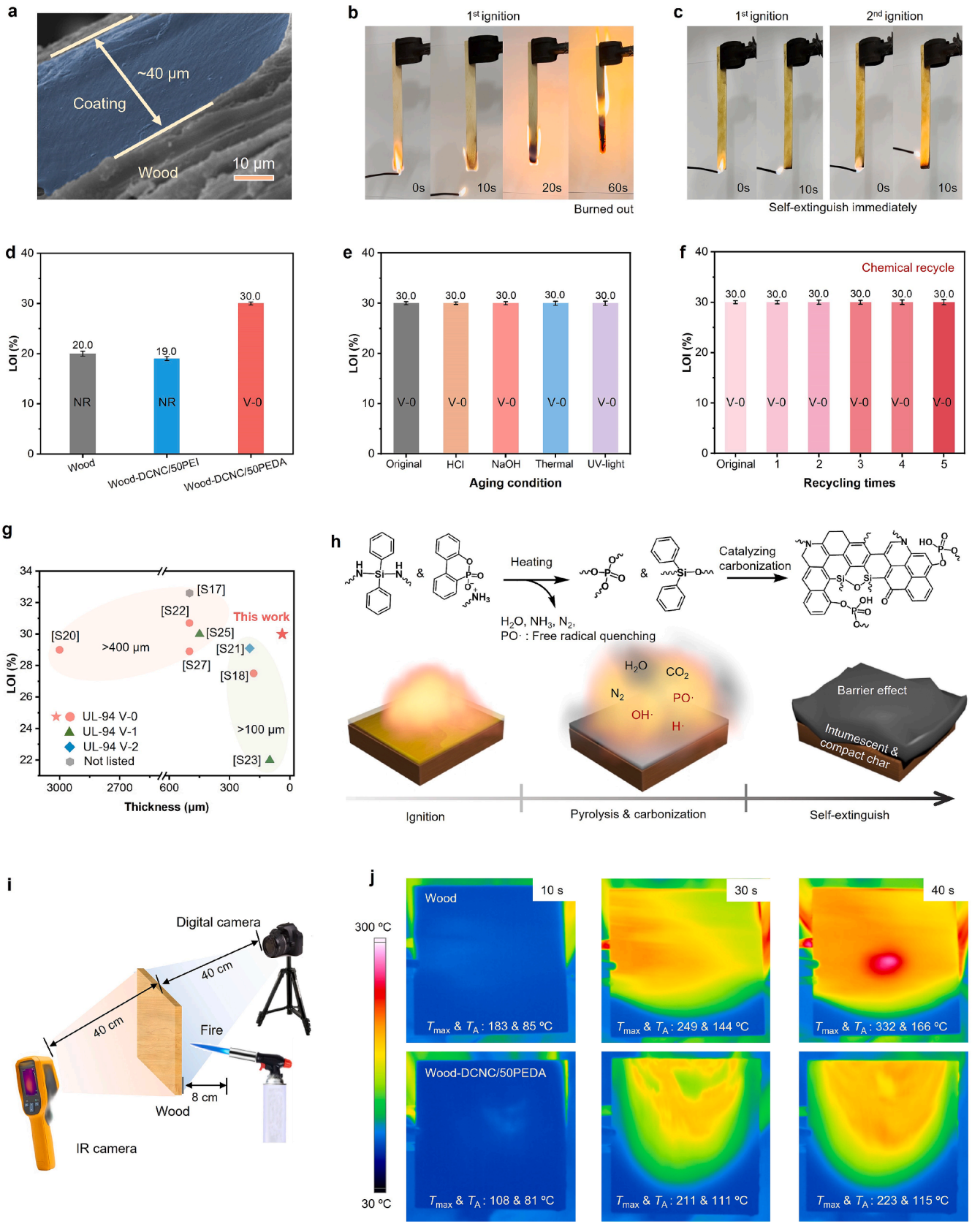

Fig. 5. The fire retardancy of DCNC/50PEDA coating on wood. (a) SEM image of DCNC/50PEDA coating applied to wood; combustion processes of (b) uncoated wood and (c) Wood-DCNC/50PEDA in UL-94 tests. (d) LOI values and UL-94 ratings of wood, Wood-DCNC/50PEI, and Wood-DCNC/50PEDA. (e) LOI and UL-94 results after different aging tests. (f) LOI and UL-94 results of coated wood after different chemical recycling cycles. (g) comparison of LOI value, UL-94 rating and coating thickness of Wood-DCNC/50PED and previous flame retardant-coated woods. (h) schematic illustration for the flame-retardant mechanism of DCNC/

PEDA on wood. (i) schematic diagram of the fire impact test. and (j) the infrared thermal images of the backside for wood and Wood-DCNC/50PEDA during fire impact tests.

40 μm (see Fig. 5g and Table S7).

It is important to elucidate the modes of action of DCNC/50PEDA as a fire-retardant coating. Compared to wood, the peak heat release rate (PHRR) and total heat release (THR) of the DCNC/50PEDA-coated wood are decreased by 23.4 and 20.2%, respectively (see Fig. S28 and Table S8). The DCNC/50PEDA-coated wood exhibits a decreased average effective heat of combustion (AEHC) and a significantly increased char residue compared to the uncoated wood (see Fig. S28c and Table S8), suggesting the condensed/gas-phase fire retardant mechanisms of DCNC/50PEDA, which can be further confirmed by other tests (see Fig. S29-S32 and Table S9). Basically, DCNC/50PEDA can suppress the combustion reaction and improve the fire retardancy of wood by releasing inert gases and P-containing radicals with diluting and radical-quenching effects in the gas phase and forming a compact and intumescent char to prevent heat and oxygen transfer on the wood surface (see Fig. 5h) [62].

A relatively simple fire test was developed to visualize the thermal protection of wood coated with DCNC/50PEDA during burning (see Fig. 5i). An infrared thermography camera was used to record the maximum temperature (T_{max}) and average temperature (T_A) of the backside of wood when its frontside (coated side) is continuously exposed to high-temperature flames (1200–1300 °C). Both T_{max} and T_A of Wood-DCNC/50PEDA are much lower than those of wood within 40 s (see Fig. 5j). Additionally, the backside temperature of the coated wood or Wood-DCNC/50PEDA is only 115 °C at 40 s because of the compact char layer formed on the wood surface that can effectively prevent heat transfer and protect the underlying wood substrate.

4. Conclusion

In summary, this work provides a facile yet promising complementary dynamic design strategy to fabricate a high-performance epoxy vitrimer which features a unique combination of room-temperature self-healing, closed-loop recyclability, superior mechanical, adhesive and fire-retardant performances. Because of the dynamic H-bonds, π-π stacking, and β-hydroxyesters within the network of the hyperbranched DCNC/50PEDA vitrimer, it shows a high self-healing efficiency of 96.0% at R.T. and maintains excellent self-healing performances after experiencing a range of mechanical damage. Also, it has high tensile strength (~36.0 MPa) and excellent intrinsic flame-retardant performances (e.g., LOI: 39.0%, and UL-94 V-0 rating), which is superior to previous room-temperature self-healing polymers. Finally, the DCNC/50PEDA exhibits excellent recyclability and degradability. Such a performance portfolio enables as-developed DCNC/50PEDA to hold great potential for many important applications in industries, such as construction, coatings, and adhesives.

CRediT authorship contribution statement

Cheng Wang: Writing – original draft, Visualization, Investigation. **Siqi Huo:** Writing – review & editing, Supervision, Project administration, Conceptualization. **Guofeng Ye:** Formal analysis. **Qi Zhang:** Data curation. **Cheng-Fei Cao:** Resources. **Mark Lynch:** Validation. **Hao Wang:** Supervision. **Pingan Song:** Writing – review & editing, Visualization. **Zhitian Liu:** Supervision, Project administration.

Declaration of competing interest

The authors declare that they have no known competing financial interests or personal relationships that could have appeared to influence the work reported in this paper.

Acknowledgements

This work was financially supported by Australian Research Council (Grant Nos. DE230100616, FT190100188, LP230100278, DP240102628, and DP240102728), Foundation for Outstanding Youth Innovative Research Groups of Higher Education Institution in Hubei Province (T201706), and Foundation for Innovative Research Groups of Hubei Natural Science Foundation of China (2017CFA009).

Appendix A. Supplementary data

Supplementary data to this article can be found online at https://doi.org/10.1016/j.cej.2024.157418.

Data availability

Data will be made available on request.

References

[1] Y. Ding, Z. Pang, K. Lan, Y. Yao, G. Panzarasa, L. Xu, M. Lo Ricco, D. R. Rammer, J. Y. Zhu, M. Hu, X. Pan, T. Li, I. Burgert, L. Hu, Emerging Engineered Wood for Building Applications, Chem. Rev. 123 (2022) 1843-1888. https://doi.org/10.1021/acs.chemrev.2c00450.
[2] J.H. Shin, M.B. Yi, T.H. Lee, H.J. Kim, Rapidly Deformable Vitrimer Epoxy System with Supreme Stress-Relaxation Capabilities via Coordination of Solvate Ionic Liquids, Adv. Funct. Mater. 32 (2022) 2207329, https://doi.org/10.1002/adfm.202207329.
[3] W. Denissen, J.M. Winne, F.E. Du Prez, Vitrimers: permanent organic networks with glass-like fluidity, Chem. Sci. 7 (2015) 30–38, https://doi.org/10.1039/c5sc02223a.
[4] Z. Zhang, D. Lei, C. Zhang, Z. Wang, Y. Jin, W. Zhang, X. Liu, J. Sun, Strong and Tough Supramolecular Covalent Adaptable Networks with Room-Temperature Closed-Loop Recyclability, Adv. Mater. 35 (2022) 2208619, https://doi.org/10.1002/adma.202208619.
[5] W. Zou, J. Dong, Y. Luo, Q. Zhao, T. Xie, Dynamic Covalent Polymer Networks: from Old Chemistry to Modern Day Innovations, Adv. Mater. 29 (2017) 1606100, https://doi.org/10.1002/adma.201606100.
[6] W. Gu, F. Li, T. Liu, S. Gong, Q. Gao, J. Li, Z. Fang, Recyclable, Self-Healing Solid Polymer Electrolytes by Soy Protein-Based Dynamic Network, Adv. Sci. 9 (2022) 2103623, https://doi.org/10.1002/advs.202103623.
[7] Y. Yang, Y. Xu, Y. Ji, Y. Wei, Functional epoxy vitrimers and composites, Prog. Mater. Sci. 120 (2021) 100710, https://doi.org/10.1016/j.pmatsci.2020.100710.
[8] C.M. Hamel, X. Kuang, K.J. Chen, H.J. Qi, Reaction-Diffusion Model for Thermosetting Polymer Dissolution through Exchange Reactions Assisted by Small-Molecule Solvents, Macromolecules 52 (2019) 3636–3645, https://doi.org/10.1021/acs.macromol.9b00540.
[9] K. Yu, Q. Shi, M.L. Dunn, T. Wang, H.J. Qi, Carbon Fiber Reinforced Thermoset Composite with Near 100% Recyclability, Adv. Funct. Mater. 26 (2016) 6098–6106, https://doi.org/10.1002/adfm.201602056.
[10] D. Montarnal, M. Capelot, F. Tournilhac, L. Leibler, Silica-Like Malleable Materials from Permanent Organic Networks, Science 334 (2011) 965–968, https://doi.org/10.1126/science.1212648.
[11] X. Wu, X. Yang, R. Yu, X.-J. Zhao, Y. Zhang, W. Huang, A facile access to stiff epoxy vitrimers with excellent mechanical properties via siloxane equilibration, J. Mater. Chem. A 6 (2018) 10184–10188, https://doi.org/10.1039/c8ta02102c.
[12] S. Chappuis, P. Edera, M. Cloitre, F. Tournilhac, Enriching an Exchangeable Network with One of Its Components: The Key to High-Tg Epoxy Vitrimers with Accelerated Relaxation, Macromolecules 55 (2022) 6982–6991, https://doi.org/10.1021/acs.macromol.2c01005.
[13] J. Han, T. Liu, C. Hao, S. Zhang, B. Guo, J. Zhang, A Catalyst-Free Epoxy Vitrimer System Based on Multifunctional Hyperbranched Polymer, Macromolecules 51 (2018) 6789–6799, https://doi.org/10.1021/acs.macromol.8b01424.
[14] Y. Xu, S. Dai, J. Bi, J. Jiang. H. zhang, Y. Chen, Catalyst-free self-healing bio-based vitrimer for a recyclable, reprocessable, and self-adhered carbon fiber reinforced composite, Chem. Eng. J. 429 (2021) 132518. https://doi.org/10.1016/j.cej.2021.132518.
[15] J. Liu, C.S.Y. Tan, Z. Yu, N. Li, C. Abell, O.A. Scherman, Tough Supramolecular Polymer Networks with Extreme Stretchability and Fast Room-Temperature Self-Healing, Adv. Mater. 29 (2017) 1605325, https://doi.org/10.1002/adma.201605325.
[16] B. Li, P.F. Cao, T. Saito, A.P. Sokolov, Intrinsically Self-Healing Polymers: From Mechanistic Insight to Current Challenges, Chem. Rev. 123 (2023) 701–735, https://doi.org/10.1021/acs.chemrev.2c00575.

[17] Y. Wang, X. Huang, X. Zhang, Ultrarobust, tough and highly stretchable self-healing materials based on cartilage-inspired noncovalent assembly nanostructure, Nat. Commun. 12 (2021) 1291, https://doi.org/10.1038/s41467-021-21577-7.

[18] Y. Yang, E.M. Terentjev, Y. Wei, Y. Ji, Solvent-assisted programming of flat polymer sheets into reconfigurable and self-healing 3D structures, Nat. Commun. 9 (2018) 1906, https://doi.org/10.1038/s41467-018-04257-x.

[19] S. Wang, M.W. Urban, Self-healing polymers, Nat. Rev. Mater. 5 (2020) 562–583, https://doi.org/10.1038/s41578-020-0202-4.

[20] Q. Zhang, C.-Y. Shi, D.-H. Qu, Y.-T. Long, B.L. Feringa, H. Tian, Exploring a naturally tailored small molecule for stretchable, self-healing, and adhesive supramolecular polymers, Sci. Adv. 4 (2018) eaat8192, https://doi.org/10.1126/sciadv.aat8192.

[21] Y.M. Li, Z.P. Zhang, M.Z. Rong, M.Q. Zhang, Tailored modular assembly derived self-healing polythioureas with largely tunable properties covering plastics, elastomers and fibers, Nat. Commun. 13 (2022) 2633, https://doi.org/10.1038/s41467-022-30364-x.

[22] N. Wang, X. Yang, X. Zhang, Ultrarobust subzero healable materials enabled by polyphenol nano-assemblies, Nat. Commun. 14 (2023) 814, https://doi.org/10.1038/s41467-023-36461-9.

[23] Z. Ma, J. Feng, S. Huo, Z. Sun, S. Bourbigot, H. Wang, J. Gao, L.-C. Tang, W. Zheng, P. Song, S.-H. Mussel-Inspired, Highly Effective Fully Polymeric Fire-Retardant Coatings Enabled by Group Synergy, Adv. Mater. (2024) 2410453, https://doi.org/10.1002/adma.202410453.

[24] Y. Xue, M. Zhang, S. Huo, Z. Ma, M. Lynch, B.T. Tuten, Z. Sun, W. Zheng, Y. Zhou, P. Song, Engineered Functional Segments Enabled Mechanically Robust, Intrinsically Fire-Retardant, Switchable, Degradable PolyureThane Adhesives, Adv. Funct. Mater. (2024) 2409139, https://doi.org/10.1002/adfm.202409139.

[25] C. Wang, S. Huo, G. Ye, P. Song, H. Wang, Z. Liu, A P/Si-containing polyethylenimine curing agent towards transparent, durable fire-safe, mechanically-robust and tough epoxy resins, Chem. Eng. J. 451 (2023) 138768, https://doi.org/10.1016/j.cej.2022.138768.

[26] C. Wang, S. Huo, G. Ye, B. Wang, Z. Guo, Q. Zhang, P. Song, H. Wang, Z. Liu, Construction of an epoxidized, phosphorus-based poly(styrene butadiene styrene) and its application in high-performance epoxy resin, Compos. b. Eng. 268 (2024) 111075, https://doi.org/10.1016/j.compositesb.2023.111075.

[27] S.Q. Huo, P.A. Song, B. Yu, S.Y. Ran, V.S. Chevali, L. Liu, Z.P. Fang, H. Wang, Phosphorus-containing flame retardant epoxy thermosets: Recent advances and future perspectives, Prog. Polym. Sci. 114 (2021) 101366, https://doi.org/10.1016/j.progpolymsci.2021.101366.

[28] S.Q. Huo, T. Sai, S.Y. Ran, Z.H. Guo, Z.P. Fang, P.G. Song, H. Wang, A hyperbranched P/N/B-containing oligomer as multifunctional flame retardant for epoxy resins, Compos. b. Eng. 234 (2022) 109701, https://doi.org/10.1016/j.compositesb.2022.109701.

[29] S. Huo, Z. Zhou, J. Jiang, T. Sai, S. Ran, Z. Fang, P. Song, H. Wang, Flame-retardant, transparent, mechanically-strong and tough epoxy resin enabled by high-efficiency multifunctional boron-based polyphosphonamide, Chem. Eng. J. 427 (2022) 131578, https://doi.org/10.1016/j.cej.2021.131578.

[30] J. Zhou, H. Liu, Y. Sun, C. Wang, K. Chen, Self-Healing Titanium Dioxide Nanocapsules-Graphene/Multi-Branched Polyurethane Hybrid Flexible Film with Multifunctional Properties toward Wearable Electronics, Adv. Funct. Mater. 31 (2021) 2011133, https://doi.org/10.1002/adfm.202011133.

[31] S.M. Kim, H. Jeon, S.H. Shin, S.A. Park, J. Jegal, S.Y. Hwang, D.X. Oh, J. Park, Superior Toughness and Fast Self-Healing at Room Temperature Engineered by Transparent Elastomers, Adv. Mater. 30 (2017) 1705145, https://doi.org/10.1002/adma.201705145.

[32] L. Zhang, Z. Liu, X. Wu, Q. Guan, S. Chen, L. Sun, Y. Guo, S. Wang, J. Song, E. M. Jeffries, C. He, F.L. Qing, X. Bao, Z. You, A Highly Efficient Self-Healing Elastomer with Unprecedented Mechanical Properties, Adv. Mater. 31 (2019) e1901402.

[33] H. Wang, Y. Yang, M. Nishiura, Y. Higaki, A. Takahara, Z. Hou, Synthesis of Self-Healing Polymers by Scandium-Catalyzed Copolymerization of Ethylene and Anisylpropylenes, J Am Chem. Soc. 141 (2019) 3249–3257, https://doi.org/10.1021/jacs.8b13316.

[34] X. Zhu, W. Zheng, H. Zhao, L. Wang, Non-covalent assembly of a super-tough, highly stretchable and environmentally adaptable self-healing material inspired by nacre, J. Mater. Chem. A 9 (2021) 20737–20747, https://doi.org/10.1039/d1ta05483j.

[35] Y. Li, W. Li, A. Sun, M. Jing, X. Liu, L. Wei, K. Wu, Q. Fu, A self-reinforcing and self-healing elastomer with high strength, unprecedented toughness and room-temperature reparability, Mater. Horizons 8 (2021) 267–275, https://doi.org/10.1039/d0mh01447h.

[36] H. Park, T. Kang, H. Kim, J.-C. Kim, Z. Bao, J. Kang, Toughening self-healing elastomer crosslinked by metal–ligand coordination through mixed counter anion dynamics, Nat. Commun. 14 (2023) 5026, https://doi.org/10.1038/s41467-023-40791-z.

[37] Q. Zhao, M. Zhang, S.S. Gao, Z. Pan, Y.J. Xue, P.Y. Jia, C.Y. Bo, Z.Y. Luo, F. Song, Y. H. Zhou, A mussel-inspired high bio-content thermosetting polyimine polymer with excellent adhesion, flame retardancy, room-temperature self-healing and diverse recyclability, J. Mater. Chem. A 10 (2022) 11363–11374, https://doi.org/10.1039/d2ta01062c.

[38] J. Peng, S. Xie, T. Liu, D. Wang, R. Ou, C. Guo, Q. Wang, Z. Liu, High-performance epoxy vitrimer with superior self-healing, shape-memory, flame retardancy, and antibacterial properties based on multifunctional curing agent, Compos. b. Eng. 242 (2022) 110109, https://doi.org/10.1016/j.compositesb.2022.110109.

[39] X. Shang, Y. Jin, W. Du, L. Bai, R. Zhou, W. Zeng, K. Lin, Flame-Retardant and Self-Healing Waterborne Polyurethane Based on Organic Selenium, ACS Appl. Mater. Interfaces. 15 (2023) 16118–16131, https://doi.org/10.1021/acsami.3c02251.

[40] S. Gao, J. Ding, W. Wang, J. Lu, MXene based flexible composite phase change material with shape memory, self-healing and flame retardant for thermal management, Compos. Sci. Technol. 234 (2023) 109945, https://doi.org/10.1016/j.compscitech.2023.109945.

[41] Y. Mao, S. Shi, L. Lei, C. Wang, D. Wang, J. Hu, S. Fu, A self-healable and highly flame retardant TiO_2@MXene/P, N-containing polyimine nanocomposite for dual-mode fire sensing, Chem. Eng. J. 479 (2024) 147545, https://doi.org/10.1016/j.cej.2023.147545.

[42] H. Xu, J. Ji, H. Li, J. Tu, Z. Fan, X. Zhang, X. Guo, Mechanically strong, soft yet tough, tear-resistant and room-temperature healable elastomers via dynamic biphasic hard segment strategy for flame retardant application, Chem. Eng. J. 475 (2023) 146018, https://doi.org/10.1016/j.cej.2023.146018.

[43] P. Chen, Y. Ding, Y. Wang, H. Zhao, P. Li, Y. Liu, C. Gao, Functional bio-based vitrimer with excellent healing and recyclability based on conjugated deflection self-toughening, Chem. Eng. J. 474 (2023) 145680, https://doi.org/10.1016/j.cej.2023.145680.

[44] Z.P. Zhang, M.Z. Rong, M.Q. Zhang, Self-healable functional polymers and polymer-based composites, Prog. Polym. Sci. 144 (2023) 101724, https://doi.org/10.1016/j.progpolymsci.2023.101724.

[45] X. Zhang, Q. Fu, Y. Wang, H. Zhao, S. Hao, C. Ma, F. Xu, J. Yang, Tough Liquid-Free Ionic Conductive Elastomers with Robust Adhesion and Self-Healing Properties for Ionotronic Devices, Adv. Funct. Mater. 34 (2023) 2307400, https://doi.org/10.1002/adfm.202307400.

[46] X. Zhu, W. Zhang, G. Lu, H. Zhao, L. Wang, Ultrahigh Mechanical Strength and Robust Room-Temperature Self-Healing Properties of a Polyurethane-Graphene Oxide Network Resulting from Multiple Dynamic Bonds, ACS Nano 16 (2022) 16724–16735, https://doi.org/10.1021/acsnano.2c06264.

[47] Y. Hu, S. Tong, Y. Sha, J. Yu, L. Hu, Q. Huang, P. Jia, Y. Zhou, Cardanol-based epoxy vitrimer/carbon fiber composites with integrated mechanical, self-healing, reprocessable, and welding properties and degradability, Chem. Eng. J. 471 (2023) 144633, https://doi.org/10.1016/j.cej.2023.144633.

[48] Q. Jin, R. Du, H. Tang, Y. Zhao, W. Peng, Y. Li, J. Zhang, T. Zhu, X. Huang, D. Kong, Y. He, T. Bao, D. Kong, X. Wang, R. Wang, Q. Zhang, X. Jia, Toughness and Self-healing Conductors, Angew. Chem. Int. Ed. 62 (2023) e202305282.

[49] X. Yao, S. Zhang, L. Qian, N. Wei, V. Nica, S. Coseri, F. Han, Super Stretchable, Self-Healing, Adhesive Ionic Conductive Hydrogels Based on Tailor-Made Ionic Liquid for High-Performance Strain Sensors, Adv. Funct. Mater. 32 (2022) 2204565, https://doi.org/10.1002/adfm.202204565.

[50] X. Wang, S. Zhan, Z. Lu, J. Li, X. Yang, Y. Qiao, Y. Men, J. Sun, Healable, Recyclable, and Mechanically Tough Polyurethane Elastomers with Exceptional Damage Tolerance, Adv. Mater. 17 (2020) 2005759, https://doi.org/10.1002/adma.202005759.

[51] H. Guo, X. Fang, L. Zhang, J. Sun, Facile Fabrication of Room-Temperature Self-Healing, Mechanically Robust, Highly Stretchable, and Tough Polymers Using Dual Dynamic Cross-Linked Polymer Complexes, ACS Appl. Mater. Interface 11 (2019) 33356–33363, https://doi.org/10.1021/acsami.9b11166.

[52] Y. Lai, X. Kuang, P. Zhu, M. Huang, X. Dong, D. Wang, Colorless, Transparent, Robust, and Fast Scratch-Self-Healing Elastomers via a Phase-Locked Dynamic Bonds Design, Adv. Mater. 30 (2018) 1802556, https://doi.org/10.1002/adma.201802556.

[53] M. Liu, J. Zhong, Z. Li, J. Rong, K. Yang, J. Zhou, L. Shen, F. Gao, X. Huang, H. He, A high stiffness and self-healable polyurethane based on disulfide bonds and hydrogen bonding, Eur. Polym. J. 124 (2020) 109475, https://doi.org/10.1016/j.eurpolymj.2020.109475.

[54] X. Xu, L. Li, S.M. Seraji, L. Liu, Z. Jiang, Z. Xu, X. Li, S. Zhao, H. Wang, P. Song, Bioinspired, Strong, and Tough Nanostructured Poly(vinyl alcohol)/Inositol Composites: How Hydrogen-Bond Cross-Linking Works? Macromolecules 54 (2021) 9510–9521, https://doi.org/10.1021/acs.macromol.1c01725.

[55] Y. Xue, J. Lin, T. Wan, Y. Luo, Z. Ma, Y. Zhou, B.T. Tuten, M. Zhang, X. Tao, P. Song, Stretchable, Ultratough, and Intrinsically Self-Extinguishing Elastomers with Desirable Recyclability, Adv. Sci. (weinh) 10 (2023) e2207268.

[56] G. F. Ye, S. Q. Huo, C. Wang, Q. Shi, Z. T. Liu, H. Wang, One-step and green synthesis of a bio-based high-efficiency flame retardant for poly (lactic acid), Polym. Degrad. Stab. 192 (2021) 109696. https://doi.org/ 10.1016/j.polymdegradstab.2021.109696.

[57] M.A. Lucherelli, A. Duval, L. Avérous, Biobased vitrimers: Towards sustainable and adaptable performing polymer materials, Prog. Polym. Sci. 127 (2022) 101515, https://doi.org/10.1016/j.progpolymsci.2022.101515.

[58] J. Zhang, Z. Gong, C. Wu, T. Li, Y. Tang, J. Wu, C. Jiang, M. Miao, D. Zhang, Itaconic acid-based hyperbranched polymer toughened epoxy resins with rapid stress relaxation, superb solvent resistance and closed-loop recyclability, Green Chem. 24 (2022) 6900–6911, https://doi.org/10.1039/d2gc01541b.

[59] H. Wang, H. Liu, Z. Cao, W. Li, X. Huang, Y. Zhu, F. Ling, H. Xu, Q. Wu, Y. Peng, B. Yang, R. Zhang, O. Kessler, G. Huang, J. Wu, Room-temperature autonomous self-healing glassy polymers with hyperbranched structure, Proc. Natl. Acad. Sci. 117 (2020) 11299–11305, https://doi.org/10.1073/pnas.2000001117.

[60] L.Y. Zhong, Y.X. Hao, J.H. Zhang, F. Wei, T.C. Li, M.H. Miao, D.H. Zhang, Closed-Loop Recyclable Fully Bio-Based Epoxy Vitrimers from Ferulic Acid-Derived

Hyperbranched Epoxy Resin, Macromolecules 55 (2022) 595–607, https://doi.org/10.1021/acs.macromol.1c02247.
[61] F. Wei, J.H. Zhang, C. Wu, M. Luo, B.J. Ye, H.J. Zhang, J.S. Wang, M.H. Miao, T. C. Li, D.H. Zhang, Closed-Loop Recycling of Tough and Flame-Retardant Epoxy Resins, Macromolecules 56 (2023) 5290–5305, https://doi.org/10.1021/acs.macromol.3c00650.
[62] W. Gan, C. Chen, Z. Wang, J. Song, Y. Kuang, S. He, R. Mi, P.B. Sunderland, L. Hu, Dense, Self-Formed Char Layer Enables a Fire-Retardant Wood Structural Material, Adv. Funct. Mater. 29 (2019) 1807444, https://doi.org/10.1002/adfm.201807444.